

Visible-light-induced, autopromoted nickel-catalyzed three-component arylsulfonation of 1,3-enynes and mechanistic insights

Duo-Duo Hu¹, Qian Gao¹, Jing-Cheng Dai¹, Ru Cui¹, Yuan-Bo Li¹, Yuan-Ming Li²,
Xiao-Guo Zhou², Kang-Jie Bian¹, Bing-Bing Wu¹, Kai-Fan Zhang¹,
Xi-Sheng Wang^{1*} & Yan Li^{1*}

¹Hefei National Laboratory for Physical Sciences at the Microscale, Department of Chemistry, Center for Excellence in Molecular Synthesis of CAS, University of Science and Technology of China, Hefei 230026, China;

²Hefei National Laboratory for Physical Sciences at the Microscale and Department of Chemical Physics, University of Science and Technology of China, Hefei 230026, China

Received November 25, 2021; accepted January 6, 2022; published online February 21, 2022

A light-induced, nickel-catalyzed three-component arylsulfonation of 1,3-enynes in the absence of photocatalyst is reported. This methodology exhibited mild conditions, broad scope and high efficiency, and its synthetic utility has been demonstrated by a concise total synthesis of sulfone-containing drug molecule. Detailed mechanistic studies indicated that this light induced nickel catalysis is autopromoted by *in situ* produced allene, which plays a key role as co-ligand in the photoactive excited state Ni(I) species for the LMCT process. The detailed elucidation of this light-induced nickel catalytic cycle may shed some lights on the exploitation of new catalytic activity and establishment of novel methods.

light-induced, autopromoted, ligand to metal charge transfer, nickel, allene

Citation: Hu DD, Gao Q, Dai JC, Cui R, Li YB, Li YM, Zhou XG, Bian KJ, Wu BB, Zhang KF, Wang XS, Li Y. Visible-light-induced, autopromoted nickel-catalyzed three-component arylsulfonation of 1,3-enynes and mechanistic insights. *Sci China Chem*, 2022, 65: 753–761, <https://doi.org/10.1007/s11426-021-1193-5>

1 Introduction

Visible light catalysis is emerging as a powerful and efficient strategy to access diverse building blocks from readily available raw materials in a normally atom- and step-economic manner [1–9], and its combination with transition metal (TM) catalysis is among the prolific development of organic synthesis in the past decades [10–14]. Photo-transition metal dual catalysis has made significant progress on highly efficient carbon–carbon or carbon–heteroatom bond construction, which usually allows the multi-components coupling benefited from elegant relay of each catalytic cycle [15]. However, such methods heavily rely on the usage of

noble metal-based photocatalysts (such as Ir, Ru), which greatly limits the proliferation (large-scale) uses of such technology due to sustainability and cost issues [16,17]. Cheaper, organophotoredox catalysts have also been used in dual photoredox/Nickel catalyzed couplings, but oftentimes suffer from less stability and efficiency than their metal counterparts and fewer examples exist [18–20]. Stable, recyclable heterogeneous carbon nitride photocatalysts have shown great promise in their combinations with Nickel catalysis, but present challenges regarding the scale-up of heterogeneous photochemical processes [21–23].

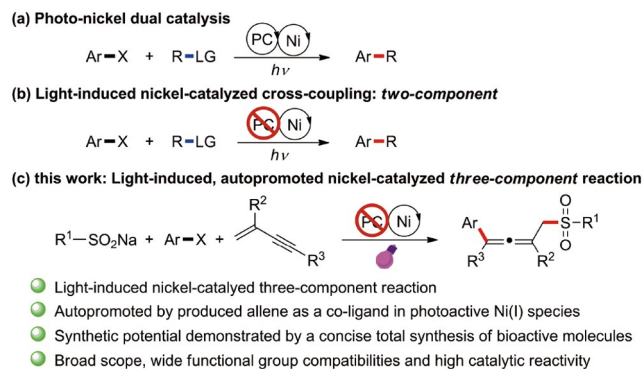
Apart from the traditional cooperative/dual photocatalysis, encouraging progress was also made with excited state transition metal-complex (Scheme 1) [24–26], especially in copper [27,28], and palladium [29], where light was only the

*Corresponding authors (email: xswang77@ustc.edu.cn; liyan08@ustc.edu.cn)

medium while excited metal-complex alone can promote subsequent reactions. Different from the conventional photo/transition metal dual catalysis, a single excited state transition metal complex is allowed to be used as both photo-absorbing species and cross-coupling catalyst for the light induced transition metal catalyzed reactions. Given the key role of ligand played in excited state transition metal catalysis, the development of new photoactive ligands for *in situ* generation of unconventional photocatalysts stands out as the biggest challenge for exploitation of new catalytic activity and establishment of novel methods. Considering the limited range and poor tunability of the photoactive ligands used in such excited state transition metal complexes, the discovery of new activation modes for the excited state transition metal catalysis could offer the best solution but far to be developed. Meanwhile the proposed mechanisms from known reports only reflect some hypotheses or are still underdeveloped, in-depth mechanistic studies are sorely needed to elucidate the activation mode for further development of new chemical transformations.

The merge of visible light induction into nickel catalysis has offered a solution to access reactive radical species under mild conditions and allowed either direct or indirect/interrupted cross-coupling of non-traditional coupling partners *via* nickel catalysis. Meanwhile photoactive ligand-containing nickel complexes have been designed and synthesized all the time, and the luminescence studies showed that this type of Ni(0) [30] or Ni(II) [31,32] complex has a long-life MLCT (metal-to-ligand charge transfer) emission at low temperatures, but not been widely used in photoredox reactions [33]. To the best of our knowledge, recently, only several cross coupling reactions [34–37] with aryl halide used as the electrophile have been developed by directly activating nickel complexes without the aid of a supplementary photocatalyst. Although the three-component reaction serves as a powerful synthetic method to construct diverse complex molecules [38–40], nevertheless, the development of three-component difunctionalization *via* light-induced nickel catalysis strategy remains undeveloped [31].

Meanwhile, sulfone compounds are famous to the sulfone therapy of leprosy [41], and also commonly found in bioactive compounds and drug molecule, such as Chlormezanone, Eletriptan, Bicalutamide, and Apremilast (Figure 1). Considering allenes served as important intermediates or precursors for further transformation to drug candidates [42–44], we hypothesized that a sulfonyl radical initiated selective arylsulfonation of 1,3-enynes might be able to furnish different molecules featuring allene moiety as a way to maximize the molecular complexity in a single step [45–48]. As the most low-cost and readily available sulfonyl source, diverse sulfinate anions could be incorporated into organic molecules *via* radical-involved sulfonation by photo promoted nickel catalytic process. Specifically, light induction



Scheme 1 Visible light induced arylsulfonation difunctionalization (color online).

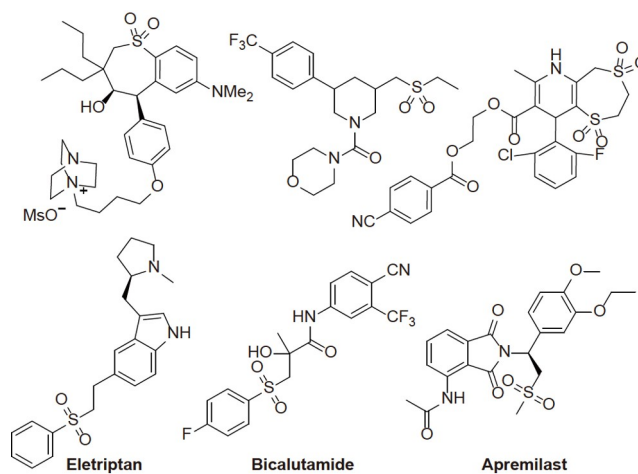


Figure 1 Sulfone containing bioactive molecules and drug molecules.

has been used to generate sulfonyl radical reductively under mild conditions and we hypothesized that this process might be utilized to promote the radical addition to unsaturated system, followed by nickel catalyzed functionalization to realize a three-component reaction process.

Herein, we described the first example of visible light induced nickel catalyzed three component reaction in the absence of photocatalyst, in which the arylsulfonation of 1,3-enynes furnished sulfone-containing allenes as important intermediates or precursors to maximize the molecular complexity in a single step [49,50]. This method exhibits mild conditions, broad substrate scope and high efficiency, and synthetic potential of this approach has also been demonstrated by a concise total synthesis of biologically active compounds. In-depth mechanistic studies indicated that this light induced nickel catalysis is autopromoted by *in situ* produced allene, which plays a key role as co-ligand in the photoactive excited state Ni(I) species for the ligand-to-metal charge transfer (LMCT) process. The detailed elucidation of this light induced nickel catalytic cycle sheds lights on the exploitation of new catalytic activity and establishment of novel methods.

2 Results and discussion

2.1 Reaction optimization

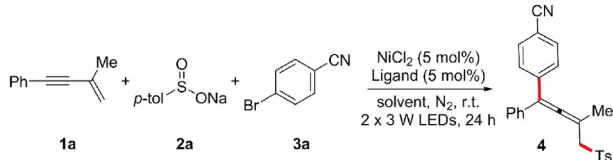
Considering electron-poor arene can act as a neutral electron acceptor, sulfinate anion could transform to sulfone radical *via* photoinduced electron transfer without supplementary photocatalyst [51]. Our investigation was initiated with 1,3-enyne **1a** as the model substrates, sodium 4-methylbenzenesulfinate **2a** as the radical source, and 4-bromobenzonitrile **3a** as the coupling partner in the presence of a catalytic amount of NiCl₂ (5 mol%) under blue light-emitting diode (LED) irradiation. To our delight, 1,3-enyne could interrupt the direct coupling of sulfinate **2a** and aryl bromide **3a**, giving sulfone-containing allenes in the yield of 5%–16% initially (entry 1, Table 1). Solvent screening reveals that this reaction cannot be carried out successfully in most solvents, while *N,N*-dimethylformamide (DMF) gave the best yield (7%–35%, entry 2). Subsequently, the investigation of light source demonstrated that a better and stable yield (83%) could be obtained under the irradiation of purple light (entry 3). Given that the rate matching and the ligands coordinating onto the metal center could tune its activity, different Ni catalysts and several ligands were then surveyed, showing that pre-synthesized NiCl₂•dtbpy complex gave a slightly better result (entries 4–12). Control experiments suggested that nickel catalyst, ligand, and light were all crucial to this three-component difunctionalization, and no product was observed in the absence of any of them (entries 14–16).

2.2 Substrate scope

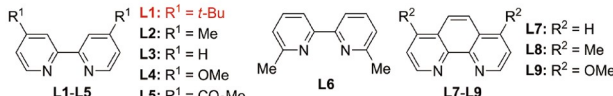
With the optimized reaction conditions in hand, we first examined the scope of the sodium sulfonates (Table 2). Electron-donating and electron-withdrawing substituted aryl sodium sulfonates **2** all worked well in this transformation, furnishing the difunctionalized products with moderate to good yields. It should be noted that sodium 4-bromobenzenesulfinate (**10**) was compatible with this catalytic system ideally, and none of the coupling byproduct from 4-sulfone phenyl bromide can be detected. The remaining bromine would be synthetic useful to construct more complex molecules *via* known transition-metal catalyzed cross-coupling reactions. Moreover, the fused ring (**12**) and heterocycle (**13**) sulfonates were also suitable to this reaction. Furthermore, sodium alkyl sulfonates, such as methyl (**14**) and cyclopropyl (**15**), also showed high reactivity in this three-component reaction, giving the corresponding difunctionalized products in 85% and 79% yield, respectively.

Next, the scope of aryl halides was investigated in this visible light induced protocol (Table 2). A series of aryl bromides embedding electron-withdrawing substituents, such as ester (**16**), acetyl (**17**), sulfone (**18**), and trifluoromethyl (**19**), at the *para*-position of phenyl rings pro-

Table 1 Optimization of conditions^{a)}



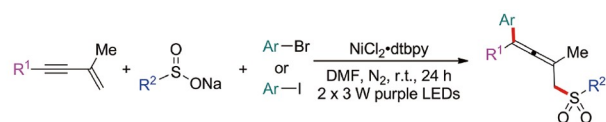
Entry	[Ni]	L	Light ^{b)}	Solvent	Yield (%) ^{c)}
1	NiCl ₂	L1	Blue	DMSO	5–16
2	NiCl ₂	L1	Blue	DMF	7–35
3	NiCl ₂	L1	Purple	DMF	83
4	NiCl ₂	L2	Purple	DMF	74
5	NiCl ₂	L3	Purple	DMF	70
6	NiCl ₂	L4	Purple	DMF	80
7	NiCl ₂	L5	Purple	DMF	14
8	NiCl ₂	L6	Purple	DMF	0
9	NiCl ₂	L7	Purple	DMF	78
10	NiCl ₂	L8	Purple	DMF	74
11	NiCl ₂	L9	Purple	DMF	72
12	NiCl ₂ •dtbpy	–	Purple	DMF	88
13	NiCl ₂ •dtbpy	–	Purple	DMSO	61
14	NiCl ₂	–	Purple	DMF	0
15	–	L1	Purple	DMF	0
16	NiCl ₂ •dtbpy	–	–	DMF	0



a) Reaction conditions: **1a** (0.4 mmol, 2.0 equiv.), **2a** (0.2 mmol, 1.0 equiv.), **3a** (0.4 mmol, 2.0 equiv.), NiCl₂ (5 mol%), dtbpy (5 mol%), DMF (2 mL), N₂, r.t., 2 × 3 W LEDs, 24 h. b) Blue LED (450–480 nm); purple LED (395–415 nm). c) ¹H NMR yield using CH₂Br₂ as internal standard.

vided the corresponding products with good to excellent yields. As for electron-neutral or electron-donating substituted substrates (**20–23**), aryl iodides are needed to carry out the reaction, obtaining 78%–92% yields of corresponding products. The *meta*-substituted aryl iodides (**24–29**) could also give good yields of the difunctionalized products. However, the iodobenzene bearing *ortho*-substitution was incompatible in this reaction system, possibly due to the steric hindrance of *ortho*-substituent to the aryl ring on the enyne. As expected, the *ortho*-substituted phenyl iodide afforded the desired allenes with good yields when the enyne substituent changed from phenyl to smaller alkyl (**30**) or H atom (**31**). Notably, this catalytic transformation could also smoothly extend to heteroaromatic iodide (**32**) by construction of pyridine-derived allene in 90% yield.

Finally, the scope of 1,3-enynes was explored by using sodium methanesulfinate and iodobenzene as coupling

Table 2 Substrate scope^{a)}

Scope of sodium sulfonates					
 4, 88% ^{b)}	 5, 72% ^{b)}	 6, 68% ^{b)}	 7, 80% ^{b)}	 8, 74% ^{b)}	 9, 34% ^{b)}
 10, 53% ^{b)}	 11, 82% ^{b)}	 12, 31% ^{b)}	 13, 63% ^{b)}	 14, 85% ^{b)}	 15, 79% ^{b)}
Scope of Aryl halides					
 14, 85% ^{b)}	 16, 73% ^{b)}	 17, 79% ^{b)}	 18, 90% ^{b)}	 19, 85% ^{b)}	 20, 88%
 21, 92%	 22, 78%	 23, 83%	 24, 77%	 25, 80%	 26, 68%
 27, 87%	 28, 94%	 29, 90%	 30, 76%	 31, 76%	 32, 90%
Scope of 1,3-enynes					
 20, 88%	 14, 75% ^{c)}	 16, 81%	 17, 84%	 19, 73%	 21, 81%
 33, 82%	 22, 82% ^{d)}	 34, 77% ^{c)}	 23, 42%	 26, 87%	 35, 87%
 27, 73%	 36, 71% ^{d)}	 37, 62%	 38, 50%	 39, 82%	 40, 88%
 41, 77%	 42, 83%	 43, 85%	 44, 86%	 45, 90%	

a) Reaction conditions: **1** (0.4 mmol, 2.0 equiv.), **2** (0.2 mmol, 1.0 equiv.), **3** (0.4 mmol, 2.0 equiv.), NiCl₂·dtbpy (5 mol%), DMF (2 mL), N₂, r.t., 2 × 3 W purple LEDs, 24 h. Isolated yield. b) Aryl bromide was used. c) 400 nm. d) 420 nm.

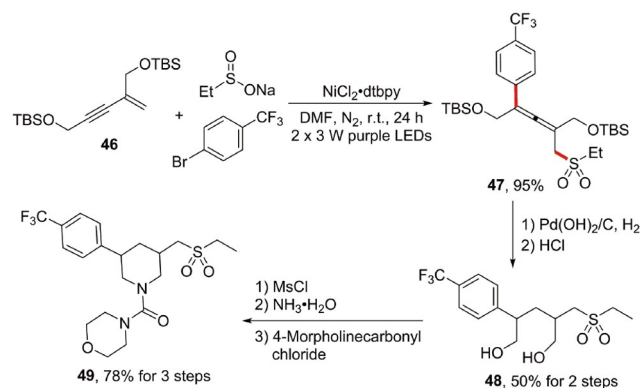
partners in order to show the universality (Table 2). An array of aryl-substituted enynes reveals little impact of the electronic effect. Electron-donating and -withdrawing substituted groups all underwent the three-component difunctionalization smoothly, delivering the desired products with good to excellent efficiency. Likely due to steric hindrance and electrical effect, the *meta*- and *ortho*-substituted enynes exhibited slightly lower reactivity, but still afforded the desired allenes in moderate to good yields. It is worth mentioning that the scope is not limited to aryl-substituted or simple alkyl-substituted (38, 44) 1,3-enynes. Sulfonamide (39), imide (40), active hydrogen (41), halide atom (42), ester (43), and heteroaromatic ring (45) could also be well tolerated and smoothly furnished good to excellent yields of allene products, which definitely demonstrated an excellent substrate scope of this three-component reaction.

2.3 Synthetic utility

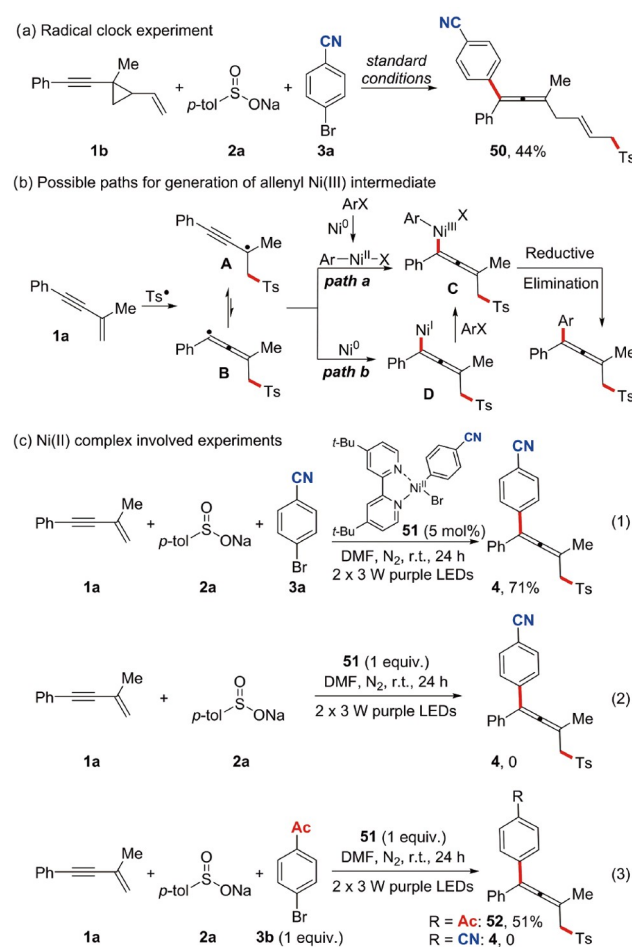
To further demonstrate the synthetic utility of this methodology, we next attempted to carry out a concise total synthesis of bioactive molecule 49 (Scheme 2) [52]. Light induced functionalization of di[(*tert*-butyldimethylsilyl)oxymethyl]enyne 46 gave the allene 47 in excellent yield. After hydrogenation and deprotection, the generated diol 48 underwent cycloamination and acylation to afford the target molecule 49. This newly developed synthetic route needs only 3 separations and with total yield of 37%.

2.4 Mechanistic studies

To gain more insight into the mechanism of this light induced transformation, a series of mechanistic studies were carried out. First, the radical clock experiment by subjection of vinyl cyclopropane 1b into standard conditions afforded the cyclo-opening allene 50 in 44% yield, which confirms the generation of sulfone radical in the catalytic cycle (Scheme 3a). Based on the previous photo-nickel dual catalysis mechanism [11–14], the trap of this sulfone radical by enyne furnished the propargyl radical A, which might isomerize to allenyl radical B and then oxidize Ni species to form Ni(III) species C via two possible paths (Scheme 3b): (1) The direct capture by Ar-Ni(II) intermediate which is *in-situ* generated by oxidative addition of aryl halide to Ni(0) (path a); (2) the trap of allene radical B by Ni(0), followed by oxidative addition of aryl halide (path b). To confirm the exact oxidation process, Ni(II) complex 51 was synthesized [53] and tested in several control experiments. As shown in Scheme 3c, while 51 can catalyze the model reaction in a comparative yield (Scheme 3c, Eq. (1)), none of the allene product 4 can be detected in the absence of aryl bromide by using 1 equiv. of 51 (Scheme 3c, Eq. (2)). Interestingly, the extra addition of 1 equiv. of 4-acetylphenyl bromide 3b afforded the 4-



Scheme 2 Total synthesis of bioactive molecule (color online).



Scheme 3 Capture of radical and Ni(II) intermediate (color online).

acetylphenyl coupling product 52 in 51% yield, but still with none of the 4-cyanophenyl coupling product 4 (Scheme 3c, Eq. (3)). Collectively, Eqs. (1) and (3) showed that Ni(II) complex 51 can transform to an activated Ni catalyst, but Eqs. (2) and (3) manifest that 51 was not a feasible intermediate in the catalytic cycle. In other words, path a (Scheme 3b) is not included in the catalytic cross-coupling cycle.

Furthermore, the intermittent irradiation experiments (Figure 2) showed that this difunctionalization undergoing effective required constant irradiation, and does not involve a light initiated radical chain process. Meanwhile, we were surprised to find that the reaction was accelerated at the next “light-on” period [54]. This phenomenon inspired us to execute a time-dependent experiment (Figure 3a). To our interests, this photoredox process behaved an obvious initial stage in the earliest 7 h (6.6% of **20**), but the yield of allene **20** has risen to 58% within 13 h in the next acceleration stage. Finally, the reaction rate slumped because of the consumption of the reactants, and the yield of **20** increased by only 3% in the last 4 h. These data clearly manifested that this reaction might involve an autocatalytic process [55]. Integrating with the previous reports [11–14] and above discussion (Scheme 3b), in view of nickel-catalyzed cross-coupling proceeds smoothly without irradiation after the generation of sulfone radical, it was speculated that this autocatalytic acceleration might be involved in the photoredox catalysis. The existence of acceleration stage proves sulfone radical will not generate through the electron transfer of sulfinate-arene. The real

photoactive substance should be generated *in situ* in the reaction system, maybe product itself or byproduct! The nuclear magnetic resonance (NMR) monitoring experiments (Figures S4–S6, in the Supporting Information online) showed catalytic amount of aryl sulfone byproduct was formed after the irradiation of sulfinate and aryl halide [56]. To examine the real photoactive substance, allene product **20** and the aryl sulfone byproduct were added into the standard conditions respectively, to observe the effect of induction period. The results indicated that the allene product **20** can promote the reaction but the aryl sulfone byproduct has no effect (Figure 3b). In addition, the induction period was inhibited after the addition of simple allene **53**, indicated that both allene and sulfone motifs are necessary to initiate this light-induced transformation.

Inspired by this result, fluorescence quenching experiments were conducted. The fluorescence of sulfonyl allene **20** can be quenched by addition of Ni(II) ($\text{NiCl}_2 \cdot \text{dtbpy}$) or Ni(I) (*in-situ* prepared by mixing equal equivalents of $\text{Ni}(\text{cod})_2$, $\text{NiCl}_2 \cdot \text{dtbpy}$, and dtbpy in anhydrous DMF) (Figure 4), which suggested that sulfonyl allene can interact with

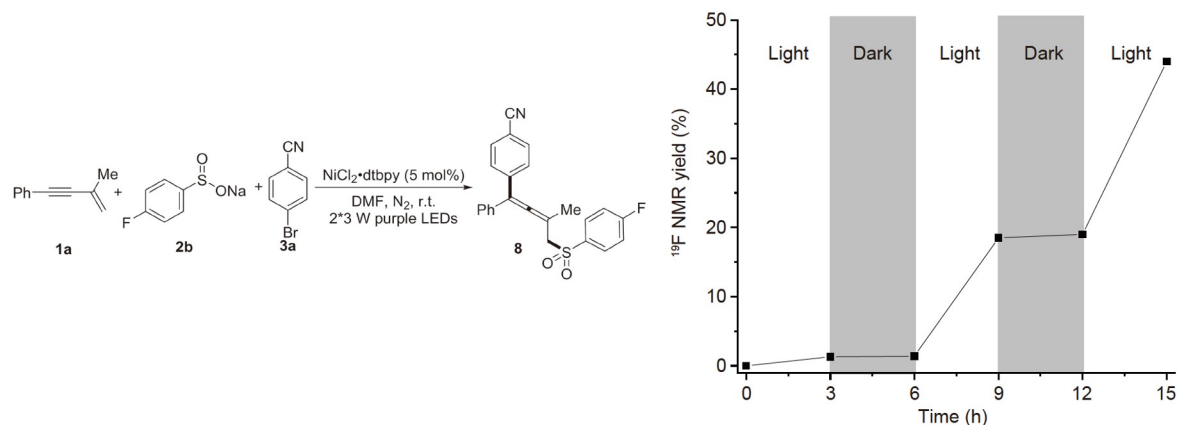


Figure 2 Light on/off experiment.

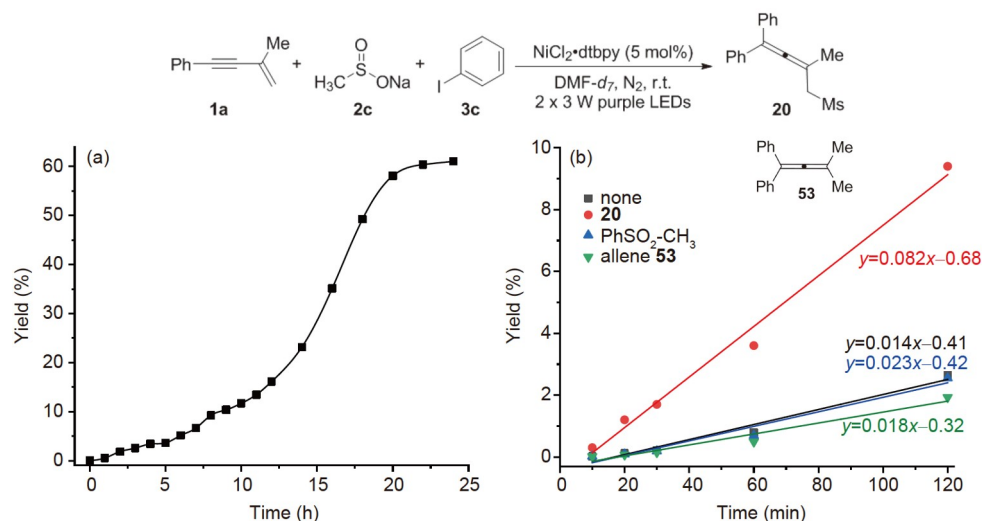


Figure 3 Rate curve. (a) Reaction progress monitoring the yield; (b) effect of additives on initial reaction rate (color online).

Ni(II) or Ni(I) under irradiation. Moreover, Stern-Volmer plots for the quenching of fluorescence intensities of **20** by Ni(II) or Ni(I) (for details, see Figures S10 and S11) gave nonlinear behaviors, indicated that the fluorescence quenching of **20** may not undergo a classical dynamic fluorescence quenching process. Finally, the transient absorption kinetic studies [57] certified that none of sulfonyl allene, Ni(II) or Ni(I) can be excited to a long-lived excited state to induce the following transformation (Figure 5a–c), but sulfonyl allene and Ni(I) can form a long-lived excited

state after pulsed laser excitation (Figure 5e) and could be quenched by sodium sulfinate (Figure 5f), which suggests a sulfonyl allene-Ni(I) LMCT excited state might be involved.

Based upon the collective mechanistic evidences and previous photo-nickel dual catalysis [11–14], a possible mechanism was suggested as shown in Scheme 4. A photoactive species, formed by sulfonyl allene **20** and Ni(I), can be excited *via* visible light irradiation, and then quenched with sodium sulfinate **2c** to generate the methylsulfone radical, Ni(0) and the free allene. The Ms• radical is then

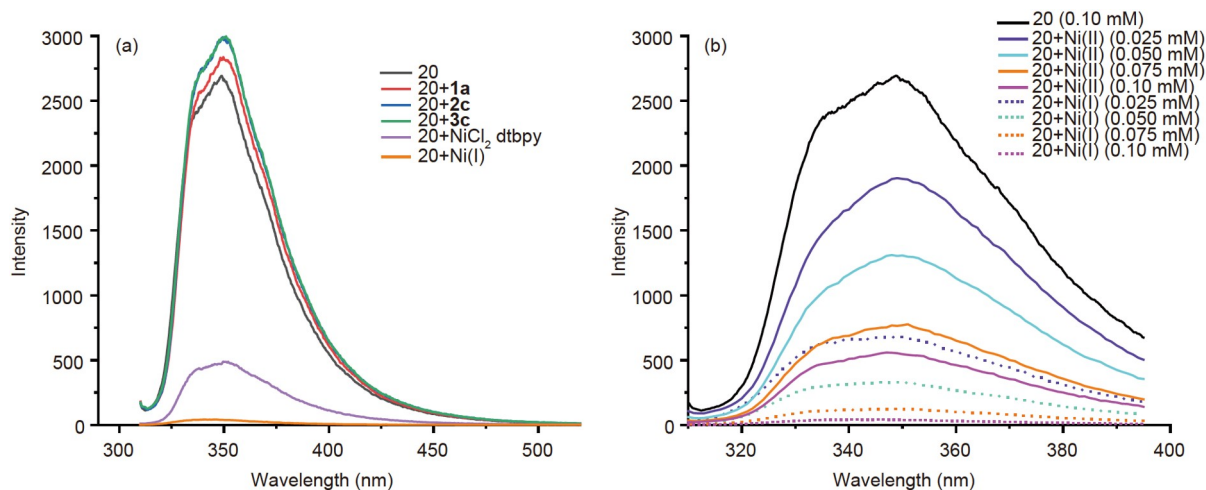


Figure 4 Fluorescence quenching experiments. (a) Emission spectra of **20** (0.1 mM) with different species (0.1 mM); (b) emission spectra of **20** (0.1 mM) at different concentrations of Ni(I) or Ni(II) (color online).

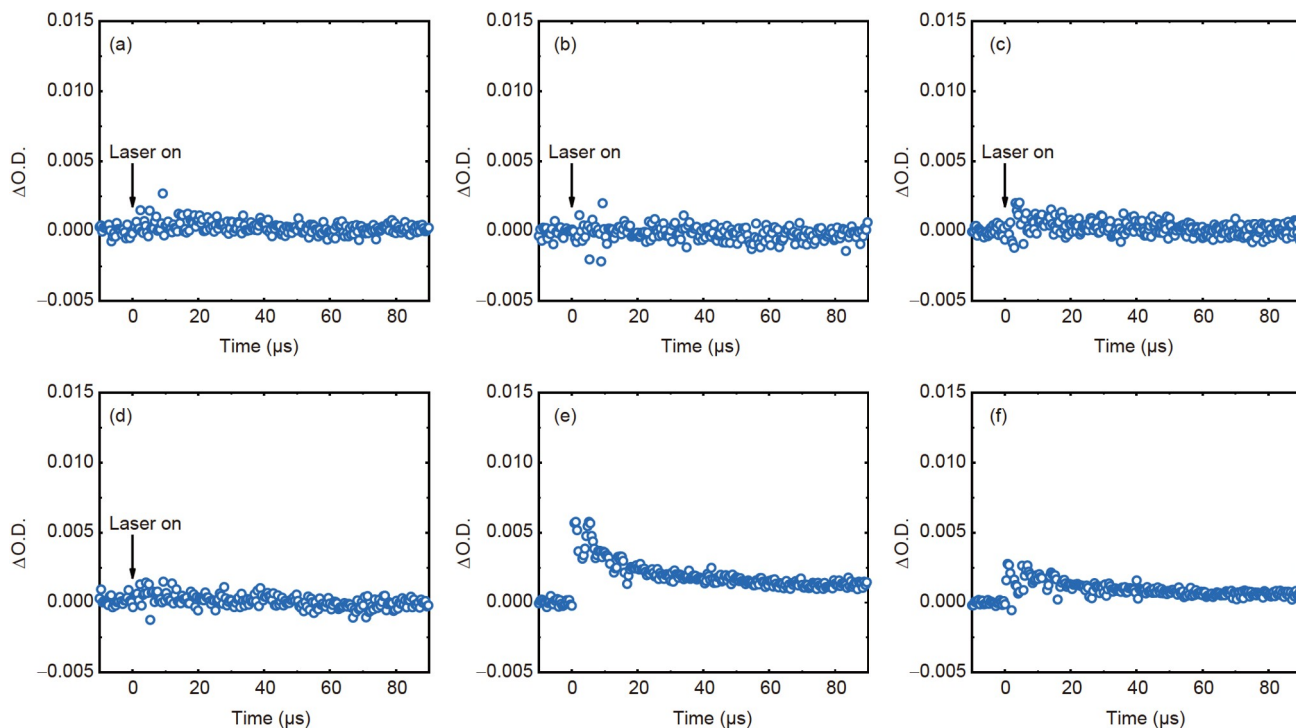
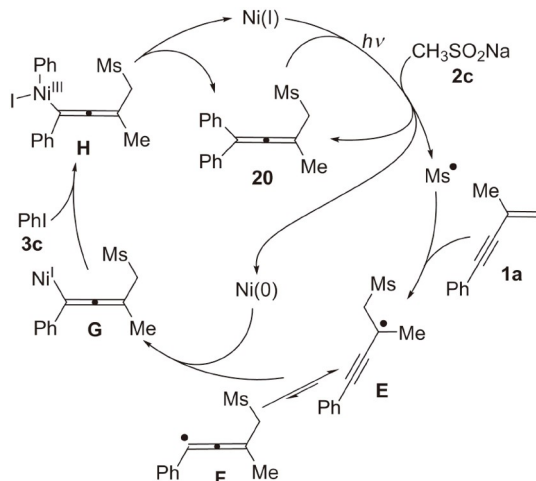


Figure 5 Transient absorption kinetics of different species at selected wavelengths following 460 nm pulsed laser excitation. (a) **20** (1 mM); (b) Ni(II) (1 mM); (c) Ni(I) (1 mM); (d) **20** (1 mM) and Ni(II) (1 mM); (e) **20** (1 mM) and Ni(I) (1 mM); (f) **20** (1 mM), Ni(I) (1 mM) and **2c** (20 mM) (color online).



Scheme 4 Probable mechanism.

captured by enyne **1a** to give a tertiary propargyl radical **E**, which can be isomerized to allenyl radical **F**. The trap of radical **F** by Ni(0) species, produced from the reduction quenching process, affords allenyl Ni(I) complex **G**. The Ni(I) complex **G** undergoes oxidative addition of PhI (**3c**), followed by reductive elimination of **H** to furnish the desired product **20**, releasing Ni(I) catalyst to enter next cycle.

3 Conclusions

In summary, we have developed a photocatalyst-free, light-induced nickel-catalyzed three component arylsulfonation of 1,3-enynes, affording sulfone-containing allenes as important intermediates or precursors to maximize the molecular complexity in a single step. This methodology demonstrates high catalytic reactivity, mild conditions and excellent functional group tolerance. The synthetic utility of this new difunctionalization was demonstrated in a concise total synthesis of the potential drug molecule. Detailed mechanistic studies support that this light induced nickel catalysis is autopromoted by produced allene as a co-ligand in the photoactive excited state Ni(I) species for the LMCT process, which shed lights on the exploitation of new catalytic activity and establishment of novel methods. Further elaboration of the mechanism and application of this light induced nickel catalytic system is currently underway in our laboratory.

Acknowledgements This work was supported by the National Science Foundation of China (21602213, 21971228).

Conflict of interest The authors declare no conflict of interest.

Supporting information The supporting information is available online at <http://chem.scichina.com> and <http://link.springer.com/journal/11426>. The

supporting materials are published as submitted, without typesetting or editing. The responsibility for scientific accuracy and content remains entirely with the authors.

- Narayanam JMR, Stephenson CRJ. *Chem Soc Rev*, 2011, 40: 102–113
- Xuan J, Xiao WJ. *Angew Chem Int Ed*, 2012, 51: 6828–6838
- Prier CK, Rankic DA, MacMillan DWC. *Chem Rev*, 2013, 113: 5322–5363
- Schultz DM, Yoon TP. *Science*, 2014, 343: 1239176
- Romero NA, Nicewicz DA. *Chem Rev*, 2016, 116: 10075–10166
- Marzo L, Pagire SK, Reiser O, König B. *Angew Chem Int Ed*, 2018, 57: 10034–10072
- Chen Y, Lu LQ, Yu DG, Zhu CJ, Xiao WJ. *Sci China Chem*, 2019, 62: 24–57
- Zhou QQ, Zou YQ, Lu LQ, Xiao WJ. *Angew Chem Int Ed*, 2019, 58: 1586–1604
- Strieth-Kalthoff F, Glorius F. *Chem*, 2020, 6: 1888–1903
- Skubi KL, Blum TR, Yoon TP. *Chem Rev*, 2016, 116: 10035–10074
- Twilton J, Le C, Zhang P, Shaw MH, Evans RW, MacMillan DWC. *Nat Rev Chem*, 2017, 1: 0052
- Milligan JA, Phelan JP, Badir SO, Molander GA. *Angew Chem Int Ed*, 2019, 58: 6152–6163
- Zhu C, Yue H, Chu L, Rueping M. *Chem Sci*, 2020, 11: 4051–4064
- Lipp A, Badir SO, Molander GA. *Angew Chem Int Ed*, 2021, 60: 1714–1726
- Garbarino S, Ravelli D, Protti S, Basso A. *Angew Chem Int Ed*, 2016, 55: 15476–15484
- Kärkäs MD, Porco Jr. JA, Stephenson CRJ. *Chem Rev*, 2016, 116: 9683–9747
- Chan AY, Perry IB, Bissonnette NB, Buksh BF, Edwards GA, Frye LI, Garry OL, Lavagnino MN, Li BX, Liang Y, Mao E, Millet A, Oakley JV, Reed NL, Sakai HA, Seath CP, MacMillan DWC. *Chem Rev*, 2021, acs.chemrev.1c00383
- Santos MS, Corrêa AG, Paixão MW, König B. *Adv Synth Catal*, 2020, 362: 2367–2372
- Qian P, Guan H, Wang YE, Lu Q, Zhang F, Xiong D, Walsh PJ, Mao J. *Nat Commun*, 2021, 12: 6613
- Zhang HH, Chen H, Zhu C, Yu S. *Sci China Chem*, 2020, 63: 637–647
- Malik JA, Madani A, Pieber B, Seeberger PH. *J Am Chem Soc*, 2020, 142: 11042–11049
- Das S, Murugesan K, Villegas Rodríguez GJ, Kaur J, Barham JP, Savateev A, Antonietti M, König B. *ACS Catal*, 2021, 11: 1593–1603
- Vijeta A, Casadevall C, Roy S, Reiser E. *Angew Chem Int Ed*, 2021, 60: 8494–8499
- Parasram M, Gevorgyan V. *Chem Soc Rev*, 2017, 46: 6227–6240
- Li Z, Jin J, Huang S. *Chin J Org Chem*, 2020, 40: 563–574
- Cheng WM, Shang R. *ACS Catal*, 2020, 10: 9170–9196
- Greaney MF. *Science*, 2016, 351: 666
- Hossain A, Bhattacharyya A, Reiser O. *Science*, 2019, 364: eaav9713
- Chuentragool P, Kurandina D, Gevorgyan V. *Angew Chem Int Ed*, 2019, 58: 11586–11598
- Malzkahn S, Wenger OS. *Coord Chem Rev*, 2018, 359: 52–56
- Grübel M, Bosque I, Altmann PJ, Bach T, Hess CR. *Chem Sci*, 2018, 9: 3313–3317
- Wong YS, Tang MC, Ng M, Yam VWW. *J Am Chem Soc*, 2020, 142: 7638–7646
- Wenger OS. *Chem Eur J*, 2021, 27: 2270–2278
- Lim CH, Kudisch M, Liu B, Miyake GM. *J Am Chem Soc*, 2018, 140: 7667–7673
- Abdiaj I, Fontana A, Gomez MV, de la Hoz A, Alcázar J. *Angew Chem Int Ed*, 2018, 57: 8473–8477
- Yang L, Lu HH, Lai CH, Li G, Zhang W, Cao R, Liu F, Wang C, Xiao J, Xue D. *Angew Chem Int Ed*, 2020, 59: 12714–12719
- Tian YM, Guo XN, Krümmenacher I, Wu Z, Nitsch J, Braunschweig H, Radius U, Marder TB. *J Am Chem Soc*, 2020, 142: 18231–18242
- Yin G, Mu X, Liu G. *Acc Chem Res*, 2016, 49: 2413–2423

- 39 Li ZL, Fang GC, Gu QS, Liu XY. *Chem Soc Rev*, 2020, 49: 32–48
- 40 Li Y, Wu D, Cheng HG, Yin G. *Angew Chem Int Ed*, 2020, 59: 7990–8003
- 41 Chang YT, Wolcott RR, Doull JA. *Med Clin N Am*, 1954, 38: 599–610
- 42 Ma S. *Chem Rev*, 2005, 105: 2829–2872
- 43 Yu S, Ma S. *Angew Chem Int Ed*, 2012, 51: 3074–3112
- 44 Blicek R, Taillefer M, Monnier F. *Chem Rev*, 2020, 120: 13545–13598
- 45 Wang F, Wang D, Zhou Y, Liang L, Lu R, Chen P, Lin Z, Liu G. *Angew Chem Int Ed*, 2018, 57: 7140–7145
- 46 Zhu X, Deng W, Chiou MF, Ye C, Jian W, Zeng Y, Jiao Y, Ge L, Li Y, Zhang X, Bao H. *J Am Chem Soc*, 2019, 141: 548–559
- 47 Zhang KF, Bian KJ, Li C, Sheng J, Li Y, Wang XS. *Angew Chem Int Ed*, 2019, 58: 5069–5074
- 48 Zeng Y, Chiou MF, Zhu X, Cao J, Lv D, Jian W, Li Y, Zhang X, Bao H. *J Am Chem Soc*, 2020, 142: 18014–18021
- 49 Chen Y, Zhu K, Huang Q, Lu Y. *Chem Sci*, 2021, 12: 13564–13571
- 50 Xu T, Wu S, Zhang QN, Wu Y, Hu M, Li JH. *Org Lett*, 2021, 23: 8455–8459
- 51 Schmalzbauer M, Marcon M, König B. *Angew Chem Int Ed*, 2021, 60: 6270–6292
- 52 Heimbach D, Roehrig S, Cancho G Y, Rester U, Bender E, Zimmermann K, Zubov D, Buchmueller A, Von Degenfeld G, Gerdes C, Gnoth MJ, Gericke KM, Jeske M. Substituted piperidines. International Patent, WO 2010/136128 A1, 2010
- 53 Zhu DL, Xu R, Wu Q, Li HY, Lang JP, Li HX. *J Org Chem*, 2020, 85: 9201–9212
- 54 Wang C, Zhang H, Wells LA, Liu T, Meng T, Liu Q, Walsh PJ, Kozlowski MC, Jia T. *Nat Commun*, 2021, 12: 932
- 55 Bissette AJ, Fletcher SP. *Angew Chem Int Ed*, 2013, 52: 12800–12826
- 56 The sulfone might be generated via the similar protocol according to: Chen L, Liang J, chen Z, Chen J, Yan M, Zhang X. *Adv Synth Catal*, 2018, adsc.201801390
- 57 Ting SI, Garakyaraghi S, Taliaferro CM, Shields BJ, Scholes GD, Castellano FN, Doyle AG. *J Am Chem Soc*, 2020, 142: 5800–5810